lubricants

MDPI

Article

Investigation of the Effects of Cutting Tool Coatings and Machining Conditions on Cutting Force, Specific Energy Consumption, Surface Roughness, Cutting Temperature, and Tool Wear in the Milling of Ti6Al4V Alloy

Barış Özlü [1], Hasan Basri Ulaş [2] and Fuat Kara [3,*]

[1] Department of Machine and Metal Technology, Technical Sciences Vocational School, Aksaray University, Aksaray 68100, Turkey
[2] Department of Manufacturing Engineering, Faculty of Technology, Gazi University, Ankara 06500, Turkey
[3] Department of Mechanical Engineering, Engineering Faculty, Düzce University, Düzce 81620, Turkey
* Correspondence: fuatkara@duzce.edu.tr

Abstract

The present study aims to investigate the effects of cutting parameters (cutting speed, Vc: 60–90–120 m/min; feed rate, f: 0.055–0.085–0.115 mm/rev), cutting tool coatings (CVD: TiN/TiCN/Al_2O_3 and PVD: TiAlN), and machining conditions (dry, air, and MQL) on cutting force (Fc), specific energy consumption (SEC), surface roughness (Ra), cutting temperature (T), and tool wear (Vb) during the milling of Ti6Al4V alloy. As a result, it was observed that all machining tests conducted with the Al_2O_3-coated cutting tool showed improvements of 4.7%, 10.75%, 3.8%, and 6.3% in Fc, SEC, Ra, and T, respectively, compared to the tests performed with the TiAlN-coated cutting tool. Under dry machining conditions, the average Fc, SEC, Ra, and T values were 302.82 N, 4.88 j/mm^3, 0.653 µm, and 241.06 °C, respectively. Compared to dry machining conditions, the air and MQL machining conditions demonstrated improvements in the average Fc by 5.15% and 6.3%, SEC by 10.27% and 17.79%, Ra by 6.23% and 11.17%, and T by 8.9% and 19.68%, respectively. The lowest Fc and Ra values for the Al_2O_3-coated cutting tool were measured at 228.33 N and 0.402 µm, respectively, under the MQL machining condition, at a cutting speed of 120 m/min and a feed rate of 0.055 mm/rev. The lowest SEC value (2.694 J/mm^3) was also obtained using the Al_2O_3-coated tool under MQL conditions at a cutting speed of 120 m/min and a feed rate of 0.115 mm/rev. Similarly, the lowest cutting temperature (129 °C) was achieved with the Al_2O_3-coated tool under MQL conditions at a cutting speed of 60 m/min and a feed rate of 0.055 mm/rev. The wear performance of the Al_2O_3-coated cutting tool was observed to be superior to that of the TiAlN-coated tool.

Keywords: Ti6Al4V alloy; minimum quantity lubrication; cutting tool coating; cutting force; specific energy consumption; surface roughness; cutting temperature; tool wear

check for updates

Received: 20 July 2025
Revised: 8 August 2025
Accepted: 12 August 2025
Published: 15 August 2025

Citation: Özlü, B.; Ulaş, H.B.; Kara, F. Investigation of the Effects of Cutting Tool Coatings and Machining Conditions on Cutting Force, Specific Energy Consumption, Surface Roughness, Cutting Temperature, and Tool Wear in the Milling of Ti6Al4V Alloy. *Lubricants* **2025**, *13*, 363. https://doi.org/10.3390/lubricants13080363

Copyright: © 2025 by the authors. Licensee MDPI, Basel, Switzerland. This article is an open access article distributed under the terms and conditions of the Creative Commons Attribution (CC BY) license (https://creativecommons.org/licenses/by/4.0/).

1. Introduction

Ti6Al4V alloy is a typical α+β dual-phase material that exhibits exceptional mechanical properties, excellent biocompatibility, and superior corrosion resistance. It also possesses other favorable attributes such as a high strength-to-weight ratio, relatively low modulus of elasticity, high yield strength, toughness, and outstanding corrosion resistance. These characteristics of Ti6Al4V make it one of the most widely used metallic materials in the

aerospace, marine, and biomedical industries [1–6]. However, the superior mechanical and chemical properties of Ti6Al4V present significant challenges during its forming and machining processes. Its high strength and chemical reactivity hinder conventional melting and casting processes, thereby increasing manufacturing costs. Moreover, its low thermal conductivity, low elastic modulus, and high affinity for tool materials contribute to rapid tool wear and poor machinability. Consequently, Ti6Al4V alloy is classified as a difficult-to-machine material [7,8]. The alloy's high hardness and thermal resistance result in elevated cutting forces during machining operations, which in turn lead to increased tool deformation and reduced tool life [9]. As such, using different cutting tool coatings and different machining conditions to improve the machining performance of difficult-to-machine materials such as Ti6Al4V provides advantages in many aspects.

Numerous experimental and analytical studies have been conducted in the literature to improve the machining performance of Ti6Al4V alloy. These studies typically involve varying input parameters and machining conditions or modifying cutting parameters and tool coatings. These studies have also examined output parameters such as cutting force, surface roughness, specific energy consumption, cutting temperature, and tool wear. The findings from this literature review are summarized in Table 1.

Table 1. Summary of the literature review.

Author(s)	Material	Machining Conditions	Cutting Tool Coating	Output Response	Summary
Seid Ahmed and Ryon (2022) [10]	Ti6Al4V	LN_2, MQL	TiAlN	Tool wear, cutting force, surface roughness, and microhardness	Compared to MQL and LN_2 cryogenic cooling, LN_2 cryogenic cooling provided the best machining results.
An et al. (2020) [11]	Ti-64, Ti-6242S, Ti-555	DRY	Uncoated, PVD (TiN), CVD (Al_2O_3)	Tool wear	Mechanical properties significantly affect machinability and tool life. PVD tools demonstrated better wear and fracture resistance than uncoated and CVD tools.
Abdullah et al. (2017) [12]	Ti6Al4V	DRY	PVD (TiAlN/AlCrN), CVD ($TiCN/Al_2O_3$)	Tool wear	PVD tools produce the least tool wear compared to CVD tools. Depth of cut is the primary factor affecting tool life, followed by cutting speed and feed rate.
Yuan et al. (2011) [13]	Ti6Al4V	DRY, WET, MQL (Room Temperature), MQL Cooling AIR (0 °C), MQL Cooling AIR (−15 °C), MQL Cooling AIR (−30 °C), MQL Cooling AIR (−45 °C)	Uncoated cemented carbide	Cutting force, flank wear, surface roughness	They observed that cutting force, tool wear, and surface roughness were significantly reduced under MQL machining conditions. MQL (−15 °C) machining conditions performed better than other temperatures.
Gajrani (2020) [14]	Ti6Al4V	DRY, MQL, Cryo-MQL	Uncoated tungsten carbide	Cutting force, surface roughness, microhardness, tool wear	As a result of milling tests, better results were obtained for cutting force, surface roughness, microhardness, and tool wear in Cryo-MQL machining conditions.
Sahoo et al. (2021) [15]	Ti6Al4V	DRY, AIR, MQL	Uncoated tungsten carbide	Cutting force, tool-tip temperature, flank wear, chip morphology, vibration	As a result of tests conducted under MQL machining conditions, it was observed that Ti6Al4V machining performance improved.

Table 1. *Cont.*

Author(s)	Material	Machining Conditions	Cutting Tool Coating	Output Response	Summary
Saravanan et al. (2021) [16]	Ti6Al4V	DRY, Flood, MQL, Multijet MQCL	Uncoated tungsten carbide	Temperature, force, surface roughness	The best results in terms of cutting temperature, cutting force, and surface roughness were obtained under MJMQCL conditions.
Jamil et al. (2021) [17]	Ti6Al4V	DRY, MQL, LN_2	Cemented tungsten carbide	Cutting temperature, P total, tool wear, surface roughness, tool life	The best machining performance was achieved with CO_2–snow, while the minimum cutting temperature was obtained with cryogenic LN_2.
An et al. (2020) [18]	Ti6Al4V	DRY, $scCO_2$, $scCO_2$-WMQL, $scCO_2$-OoWMQL	Cemented carbide	Tool wear, cutting torque, surface morphology	As a result of the machining tests, the best results for tool wear, cutting torque, and surface roughness were obtained under $scCO_2$-OoWMQL lubrication conditions.
Ramesh et al. (2009) [19]	Ti6Al4V	DRY	PVD (TiN), CVD (Al_2O_3)	Cutting temperature, chip formation	PVD and CVD tools performed similarly; CVD produced shorter chips, while PVD produced longer ones.
Shokrani et al. (2019) [20]	Ti6Al4V	Conventional Flooding, MQL, Cryogenic, Hybrid Cryogenic MQL	Solid carbide end mill	Tool life, tool wear model, surface roughness	The hybrid cryogenic MQL system showed better machining performance in machining Ti-6Al-4V alloy compared to overflow machining.
Cai et al. (2021) [21]	Ti6Al4V	DRY, $scCO_2$, $scCO_2$-wMQL, $scCO_2$-OoWMQL	Cemented carbide end mill	Milling force, cutting temperature, surface roughness, vibration	Machining tests showed that $scCO_2$-OoWMQL achieved the lowest cutting force, temperature, and surface roughness.
Bandapalli et al. (2018) [22]	Ti6Al4V	DRY	Uncoated, PVD (TiAlN), PVD (AlTiN)	Tool wear	The main wear mechanisms in micro-end mills were diffusion, oxidation, adhesion, and abrasion. In titanium alloy machining, uncoated tools outperformed AlTiN- and TiAlN-coated carbide tools.
Park et al. (2015) [23]		Flood Coolant, Nano-MQL, External Cryogenic, Internal Cryogenic, Nano-MQL + Internal Cryogenic	Solid end mill	Milling force, tool wear	They stated that Nano-MQL + Internal Cryogenic hybrid machining gives more efficient results in terms of cutting force and tool wear.
Rotella et al. (2014) [24]		DRY, Cryogenic, MQL	PVD (TiAlN)	Surface roughness, microstructure, hardness, grain refinement, phase transformation	Cryogenic machining yielded the best surface roughness, higher surface hardness, and fewer cracks compared to other methods.
Bai et al. (2019) [25]		MQL (Al_2O_3), MQL (SiO_2), MQL (MoS_2), MQL (CNTs), MQL (SiC), MQL (Graphite)	Cemented carbide	Milling force, surface roughness, surface morphology, viscosity analysis	As a result of the machining tests, the best cutting force, surface roughness, and viscosity of nanofluids were obtained from MQL (Al_2O_3).

As shown in the literature review in Table 1, most studies on the milling of Ti6Al4V alloy and other engineering materials have primarily focused on either the effect of cooling/lubrication conditions or the effect of cutting tool coatings on output parameters typically investigated in isolation. However, research that simultaneously examines the

combined effects of cutting tool coatings and machining environments on machining performance remains limited, particularly for Ti6Al4V alloy.

In this context, the novelty of the present study lies in its integrated evaluation of tool coating type and environmentally friendly machining conditions, enabling a comprehensive understanding of their combined influence on machinability. Specifically, the study investigates the milling performance of Ti6Al4V alloy using various cutting tool coatings under different machining environments, assessing their effects on cutting force, specific energy consumption, surface roughness, cutting temperature, and tool wear across a range of cutting parameters. Furthermore, ANOVA analysis was conducted to identify the most significant input parameters influencing the measured responses, thereby providing deeper insights into the complex interactions between tool coating and machining conditions.

2. Materials and Methods

2.1. Experiment Material and Cutting Inserts

Ti6Al4V alloy with dimensions of 40 × 40 × 100 mm was used in the milling experiments. The elemental composition and mechanical properties of the Ti6Al4V alloy used in the experiments are presented in Table 2.

Table 2. Elemental composition and mechanical properties of Ti6Al4V alloy.

Elements	**Al**	**V**	**Fe**	**C**	**N**	**O**	**Ti**
Weight %	6.42	4.2	0.19	0.027	0.028	0.185	Balance
Tensile Strength (MPa)		Yield Strength (MPa)		Modulus of elasticity ($\times 10^6$ MPa)		Hardness Rockwell C	
886		827		11.3		36	

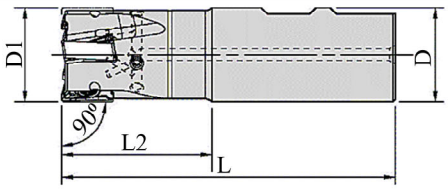
In the milling tests, two different cutting tools manufactured by Kennametal (Latrobe, PA, USA) were used: one coated with CVD (TiN/TiCN/Al_2O_3) and the other with PVD (TiAlN). A tool holder produced by the same manufacturer was also utilized. Technical specifications of the cutting tools and the tool holder used in the study are presented in Figure 1.

Cutting Tools



ISO Catalog ID	LNGU15T608SRGE
Grade	KCPK30, KC725M
Insert Length, (LI)	17.01 mm
Insert Thickness, (S)	6.96 mm
Insert Width, (W)	10 mm
Corner Facet Length, (BS)	1.8 mm
Corner Radius, (Rε)	0.8 mm

Tool Holder



ISO Catalog ID	M4D025Z02B25LN15
Effective Cutting Diameter, (D1)	25 mm
Shank Diameter, (D)	25 mm
Overall Length, (L)	89 mm
Head Length, (2)	32 mm
Number of Inserts	2

Figure 1. Cutting tools and tool holder technical information.

2.2. Experiment Material and Cutting Inserts

The milling tests were carried out on a Haas VF-2SS CNC milling machine (Oxnard, CA, USA). The cutting parameters were selected based on the recommendations provided in the cutting tool manufacturer's catalog and supported by findings from relevant literature. Three different cutting speeds and three different feed rates were employed, while the depth of cut was kept constant at 1 mm. A total of 54 experiments were performed, with a new cutting tool used for each test combination. The cutting parameters and their corresponding levels used in the experiments are presented in Table 3.

Table 3. Cutting parameters and levels for milling tests.

Milling Parameters	Levels		
	Level 1	**Level 2**	**Level 3**
Cutting tools	TiAlN	Al_2O_3	-
Machining conditions	DRY	AIR	MQL
Cutting speed, Vc (mm/min)	60	90	120
Feed rate, f (mm/rev)	0.055	0.085	0.115

2.3. Cooling Conditions

The tests were conducted under three different machining conditions. First, dry machining was performed to better understand the effects of cooling and lubrication. Second, air cooling was applied. In this condition, the CNC machine's air-cooling system, operating at 6 bar, was utilized. Third, an MQL system (Werte Mikro STN 15 model) (Istanbul, Turkey) was employed. A biostable, semi-synthetic metalworking fluid (Mackerel MS) was used as the cutting fluid. The MQL system was positioned at a 45° angle with respect to the tool axis to effectively spray the metalworking fluid into the cutting zone via a dual-nozzle setup. The spray was delivered at a pressure of 6 bar and a flow rate of 0.028 mL/s, directly targeting the primary cutting zone. This nozzle orientation was deliberately selected to ensure efficient delivery and penetration of the lubricant into the tool–chip interface, thereby improving the cooling and lubrication effects during machining. The properties of the semi-synthetic metalworking fluid are listed in Table 4.

Table 4. Technical specifications of Mackerel MS coolant.

Feature	Explanation
pH	9.5
Density (15 °C, kg/m^3)	1.070
Appearance	Clear red-brown
Smell	Typical
Yield point (°C)	−22
Refractive Index (n20/D)	1.4222

2.4. Measurements

Various devices and equipment were used to evaluate the machinability performance of the Ti6Al4V alloy. A Kistler 9257B piezoelectric dynamometer (Winterthur, Switzerland) was used to measure cutting forces during the milling tests. The signals from the dynamometer, which can simultaneously measure the three force components (Fx, Fy, and Fz), were transferred to a data acquisition card via a KISTLER 5070A multi-channel amplifier (Winterthur, Switzerland). The measured cutting force components were converted into digital values using DynoWare Version 2.4.1.3 software. A Lutron DW-6095-3 phase power

analyzer (Coopersburg, PA, USA) was employed to measure energy consumption. The power consumption of the CNC machine was measured by connecting the analyzer's current clamps separately to the three phases of the CNC machine's electrical input. A Mahr MarSurf PS 10 portable surface roughness tester (Göttingen, Lower Saxony, Germany) was used to evaluate the surface quality of the milled surfaces. Six measurements were taken from each machined surface, and the surface roughness (Ra) was determined by calculating the arithmetic mean of these values. A FLIR i60 infrared camera (Wilsonville, OR, USA) was used to measure the cutting zone temperature during machining. The average cutting temperature was calculated by averaging four individual temperature readings taken during the process. To examine tool wear and perform energy-dispersive X-ray spectroscopy (EDS) analyses, an FEI Quanta FEG 250 Scanning Electron Microscope (SEM) (Hillsboro, OR, USA) was used. The experimental setup for the study is illustrated in Figure 2.



Figure 2. Test procedure.

3. Results

3.1. Evaluation of Cutting Force

Cutting force generated during machining operations is one of the fundamental output parameters that directly affects both tool life and the surface quality of the machined part. Accurate analysis of cutting force is crucial for understanding the cutting mechanism and selecting appropriate cutting parameters. The cutting forces generated during machining are highly sensitive to machining conditions, cutting tool coatings, tool–workpiece interactions, and cutting parameters. Furthermore, the magnitude of the cutting force during machining determines both energy consumption and cutting temperature. Understanding cutting force also contributes to the development of sustainable manufacturing approaches [26–28]. In this context, the effects of cutting tool coatings and machining conditions on the cutting force during the milling of Ti6Al4V alloy were evaluated.

The effects of cutting tool coatings and machining conditions on cutting force values in the milling of Ti6Al4V alloy are shown in Figure 3. According to Figure 3, cutting force values generally ranged from 228.33 N to 886.77 N. The lowest cutting force was recorded when using the Al_2O_3-coated cutting tool under MQL machining conditions, at a cutting speed of 120 m/min and a feed rate of 0.055 mm/rev, with a value of 228.33 N. The highest cutting force was recorded with the TiAlN-coated cutting tool under dry machining conditions, at a cutting speed of 60 m/min and a feed rate of 0.115 mm/rev, reaching 886.77 N.

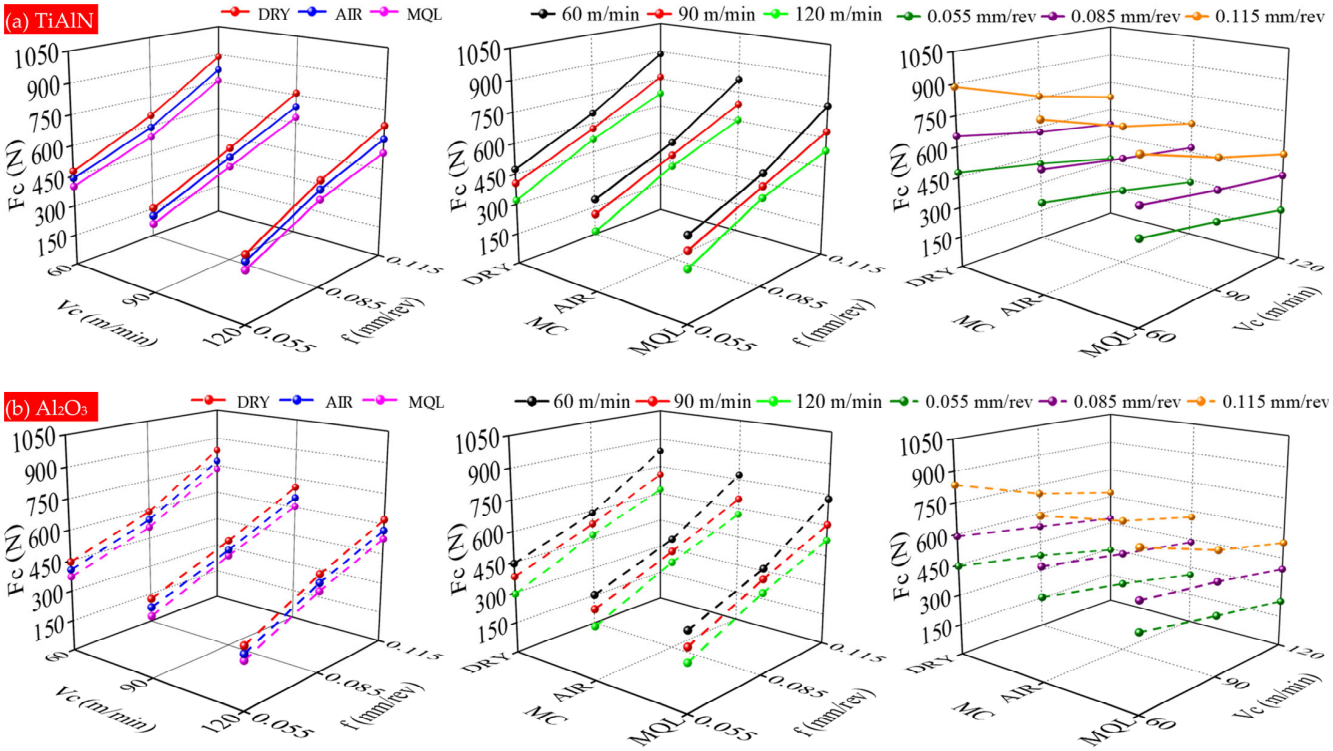


Figure 3. Cutting force results for different coating and machining conditions.

When examining the variations in cutting force with respect to cutting parameters, it is observed that the feed rate had a more significant influence on cutting force compared to cutting speed. As the feed rate increased, the volume of material removed per unit time, the degree of plastic deformation in the cutting zone, and the interaction between the tool and workpiece all increased significantly. This increase resulted in higher cutting energy requirements during the metal removal process, which in turn led to a substantial rise in the main cutting force [29].

Furthermore, the increase in cutting force with increasing feed rate, as observed in tests conducted under constant specific cutting resistance (kc) and constant depth of cut (ap), aligns well with the model described in Equation (1) [30]. On the other hand, the increase in cutting speed generally led to a reduction in cutting force. This can be attributed to the decrease in contact area at the tool–chip interface and the reduction in material shear strength due to the rise in temperature in the cutting zone [31,32].

$$Fc = kc \times ap \times f \quad (1)$$

When examining the effects of machining conditions, the average cutting force was calculated as 584.49 N in tests conducted with TiAlN-coated tools under dry machining conditions. Under air and MQL machining conditions, the cutting force was reduced by 8.82% and 17.33%, respectively, compared to dry machining. Similarly, for the Al_2O_3-coated

tool, the average cutting force under dry machining was 541.42 N. Under air and MQL conditions, the cutting force was reduced by 8.46% and 15.55%, respectively, compared to dry machining. In this context, the highest cutting forces were consistently observed under dry machining conditions for both cutting tools and all parameter combinations. Overall, lower cutting force values (by approximately 8.64%) were observed under air conditions compared to dry machining for both tool types. The application of high-pressure air to the cutting zone helped reduce the cutting temperature (Figure 6). However, the decreased temperature made it more difficult for the material to undergo plastic deformation, thereby increasing cutting forces. In contrast, the lowest cutting forces were measured under MQL machining conditions for both cutting tools. This can be attributed to the effective cooling and lubrication properties of the MQL system. The cutting fluid delivered through MQL reduced friction at the tool–workpiece interface, resulting in lower cutting forces.

For tests conducted with TiAlN-coated tools under all machining conditions and cutting parameters, the average cutting force was calculated as 533.66 N. For the Al_2O_3-coated tool, the average cutting force was 498.09 N. Accordingly, tests with the Al_2O_3-coated tool showed a 6.65% improvement in cutting force compared to the TiAlN-coated tool. Previous studies have shown that increased tool wear leads to an enlarged contact area between the tool–chip and tool–workpiece interfaces [33,34]. Therefore, the lower cutting force values and higher cutting performance observed for the Al_2O_3-coated tool can be attributed to its lower coefficient of friction and greater wear resistance.

An analysis of variance (ANOVA) was conducted to determine the effects of controllable factors, including cutting tool coating, machining conditions, cutting speed, and feed rate, on cutting force. The ANOVA was performed at a 95% confidence level, and the results are presented in Table 5. The F-values indicate the relative significance of each factor, while the contribution percentages reflect the proportion of variance explained by each factor. According to Table 5, the most influential parameter on cutting force was feed rate (74.81%), followed by cutting speed (16.81%), machining condition (5.68%), and tool coating (1.24%).

Table 5. Cutting force analysis of variance (ANOVA) results.

Cutting Parameters	DF	Seq SS	Adj SS	Adj MS	F-Value	*p*-Value	Contribution (%)
CT	1	16,980	16,980	16,980	39.32	0.000	1.24
MC	2	77,451	77,451	38,725	89.68	0.000	5.68
Vc (m/min)	2	229,343	229,343	114,672	265.55	0.000	16.81
f (mm/rev)	2	1,020,693	1,020,693	510,347	1181.84	0.000	74.81
Error	46	19,864	19,864	432			1.46
Total	53	1,364,332					100.00

3.2. Evaluation of Specific Energy Consumption

In recent years, rising specific energy consumption (SEC) and operational costs in the metalworking industry have led to increased environmental awareness and interest in energy-efficient manufacturing. Minimizing machine tool energy consumption affected by input parameters such as cutting parameters, cutting tool material, and machining conditions is crucial for improving energy efficiency and promoting sustainability, particularly in machining operations [35–37]. Therefore, in this part of the study, the effects of cutting parameters, cutting tool coating, and machining conditions on SEC during the milling of Ti6Al4V alloy were investigated.

Figure 4 shows the changes in SEC as a function of cutting parameters, cutting tool coating, and machining conditions during the milling of Ti6Al4V alloy. According to Figure 4, SEC values ranged from 2.694 J/mm^3 to 6.249 J/mm^3 across all machining tests. The minimum SEC of 2.694 J/mm^3 was obtained using an Al_2O_3-coated cutting tool under MQL conditions, at a cutting speed of 120 m/min and a feed rate of 0.115 mm/rev. The maximum SEC of 6.249 J/mm^3 was recorded with a TiAlN-coated cutting tool under dry conditions, at a cutting speed of 60 m/min and a feed rate of 0.055 mm/rev. When examining the effects of cutting speed and feed rate on SEC, it is observed that SEC generally decreases with increasing cutting speed and feed rate. At higher cutting speeds and feed rates, the cutting tool covers the machining distance more rapidly, resulting in reduced energy consumption. Therefore, high cutting speeds and feed rates significantly enhance energy efficiency by reducing machining time and SEC [38,39].

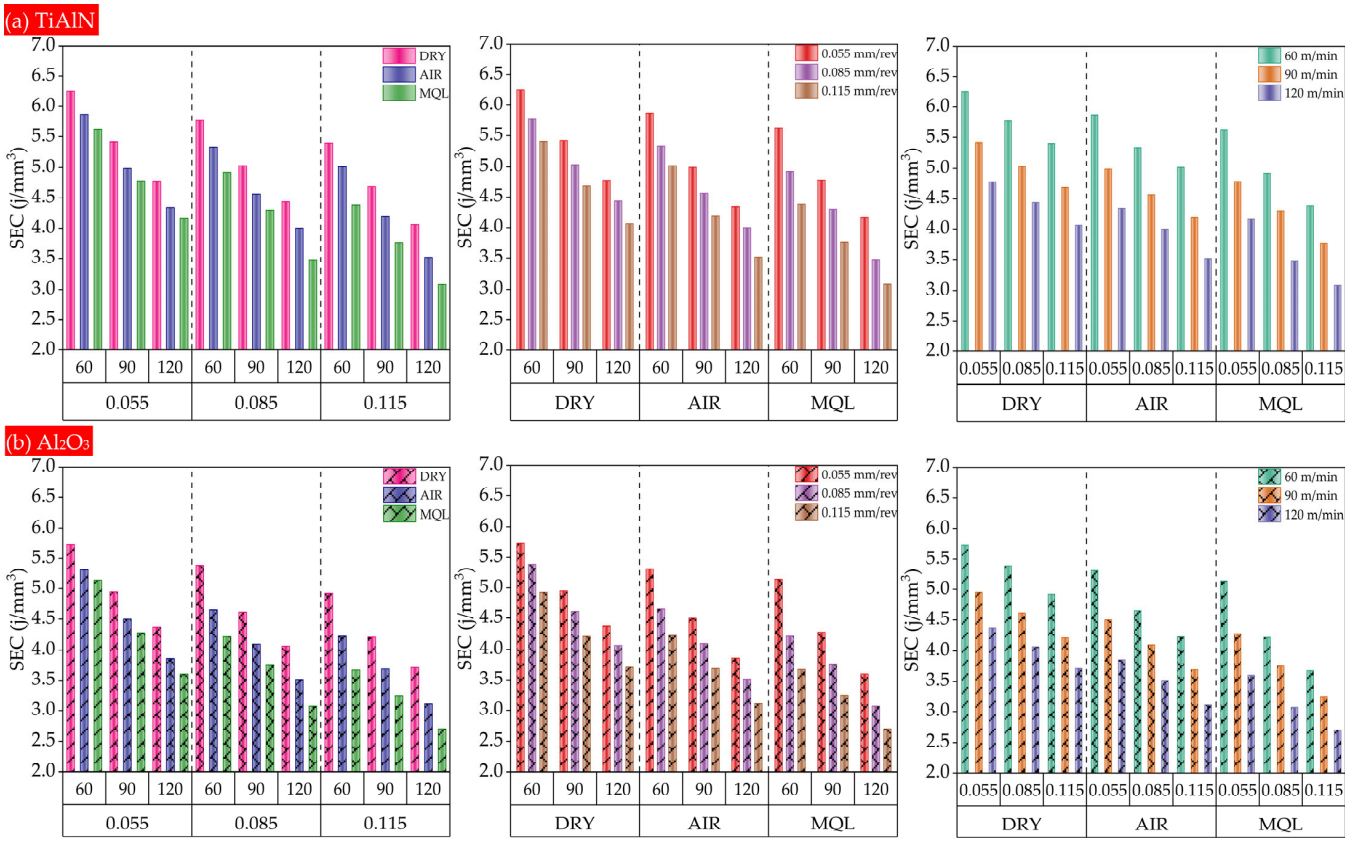


Figure 4. Specific energy consumption results for different coating and machining conditions.

In machining tests conducted with the TiAlN-coated cutting tool under all cutting parameters and machining conditions, the average SEC was calculated as 4.673 J/mm^3. When using the Al_2O_3-coated tool, SEC was reduced by 10.74%, with an average value of 4.171 J/mm^3. This improvement is attributed to the lower coefficient of friction of the Al_2O_3-coated cutting tool compared to the TiAlN-coated tool. The average SEC value under dry machining conditions was calculated as 4.879 J/mm^3 for all cutting parameters and both tool types. Under air and MQL conditions, energy efficiency improved, with SEC values decreasing by 10.27% and 17.79%, respectively, reaching 4.378 J/mm^3 and 4.011 J/mm^3. This improvement is attributed to the tribological and mechanical advantages of MQL machining. In MQL, cutting oil delivered to the cutting zone via compressed air reduces friction, facilitates chip removal, and enhances machining efficiency [40]. The lower SEC in air machining compared to dry machining can be explained by more effective cooling and reduced tool wear.

To determine the influence of cutting parameters, cutting tool coatings, and machining conditions on SEC during the milling of Ti6Al4V alloy, an analysis of variance (ANOVA) was conducted at a 95% confidence level. The results are presented in Table 6. As shown in Table 6, the most influential parameter affecting SEC was cutting speed, with a contribution rate of 46.73%, followed by feed rate (21.74%), machining conditions (19.93%), and cutting tool coating (9.92%).

Table 6. Specific energy consumption analysis of variance (ANOVA) results.

Cutting Parameters	DF	Seq SS	Adj SS	Adj MS	F-Value	*p*-Value	Contribution (%)
CT	1	3.4016	3.4016	3.40155	273.26	0.000	9.92
MC	2	6.8334	6.8334	3.41670	274.47	0.000	19.93
Vc (m/min)	2	16.0236	16.0236	8.01181	643.61	0.000	46.73
f (mm/rev)	2	7.4557	7.4557	3.72783	299.47	0.000	21.74
Error	46	0.5726	0.5726	0.01245			1.67
Total	53	34.2868					100.00

3.3. Evaluation of Surface Roughness

Figure 5 shows the effects of cutting parameters, cutting tool coating, and machining conditions on surface roughness in the milling of Ti6Al4V alloy. Figure 5 illustrates that surface roughness varied between 0.402 µm and 0.815 µm across all machining tests. The minimum surface roughness measured among machined surfaces was 0.402 µm with an Al_2O_3-coated tool under MQL machining conditions, at a cutting speed of 120 m/min and a feed rate of 0.055 mm/rev. The maximum surface roughness was 0.815 µm with a TiAlN-coated tool under dry machining conditions, at a cutting speed of 60 m/min and a feed rate of 0.115 mm/rev. As illustrated in Figure 5, at low cutting speeds, workpiece material adhering to the cutting tool is thought to increase surface roughness. As the adhering workpiece material grows, it becomes unstable and eventually fails to withstand the stresses it is subjected to during the machining process, leading to its detachment from the cutting tool. In machining, increasing cutting speeds reduces the tendency for adhering workpiece material to form, leading to a decrease in surface roughness [41,42]. Furthermore, the decrease in surface roughness values with increasing cutting speed is explained by the reduction in tool-chip contact area and friction in the tool-chip contact zone due to elevated temperatures at high cutting speeds [43,44]. On the other hand, it is observed that surface roughness values increase with increasing feed rate for both tools across all cutting parameters. Due to the increase in feed rate, surface roughness values increase as a result of greater chip volume removal per unit time. This observation is also supported by previous studies in the literature [45–48]. The surface roughness calculated for the Al_2O_3-coated cutting tool under all cutting parameters and machining conditions was 0.603 µm. This value increased by 3.93% to 0.627 µm for the TiAlN-coated cutting tool. This finding is consistent with previous studies in the literature [49].

In machining tests conducted with all cutting parameters and both cutting tools, the surface roughness was calculated as 0.653 µm under dry machining conditions. Surface roughness was reduced by 6.23% and 11.17% under air and MQL machining conditions, respectively, compared to dry machining, reaching 0.612 µm and 0.58 µm. The best surface integrity was achieved under MQL machining conditions, which reduced friction by creating a thin oil film on the tool-chip contact surface. Furthermore, the lower surface roughness under air and MQL machining conditions compared to dry machining can be explained by the enhanced cooling effect, which delays tool wear.

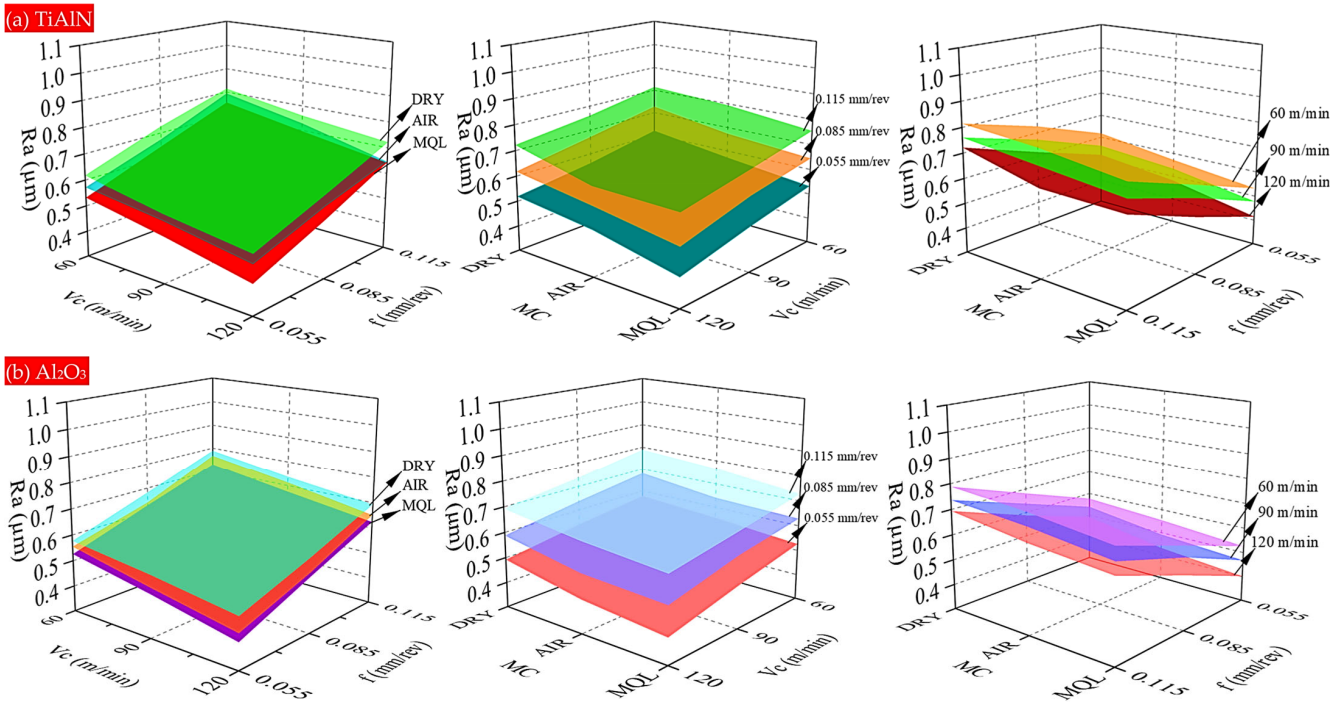


Figure 5. Surface roughness results for different coating and machining conditions.

An analysis of variance (ANOVA) was conducted to determine the effects of the controllable factors of cutting tool coating, machining conditions, cutting speed, and feed rate on surface roughness. The ANOVA analysis was performed at a 95% confidence interval. The ANOVA analysis results are shown in Table 7. As shown in Table 7, the most influential parameter on surface roughness was the feed rate with a contribution of 70.13%, followed by cutting speed with 19.05%, machining conditions with 8.65%, and cutting tool coating with 1.37%.

Table 7. Surface roughness analysis of variance (ANOVA) results.

Cutting Parameters	DF	Seq SS	Adj SS	Adj MS	F-Value	*p*-Value	Contribution (%)
CT	1	0.007585	0.007585	0.007585	78.30	0.000	1.37
MC	2	0.048029	0.048029	0.024015	247.90	0.000	8.65
Vc (m/min)	2	0.105832	0.105832	0.052916	546.25	0.000	19.05
f (mm/rev)	2	0.389584	0.389584	0.194792	2010.84	0.000	70.13
Error	46	0.004456	0.004456	0.000097			0.80
Total	53	0.555486					100.00

3.4. Evaluation of Cutting Temperature

Previous studies have reported that friction between the tool and workpiece in metalworking operations can cause high temperatures. This leads to problems such as wear, cracking, fracture, and deformation in the cutting tool, negatively impacting its life and performance. Therefore, in metalworking operations, the thermal properties of the tool, workpiece, and machining conditions, as well as the temperature generated in the cutting zone, must be thoroughly analyzed [50–52]. In this section of the study, the effects of cutting tool coating and machining conditions on the temperature in the cutting zone during the milling of Ti6Al4V alloy under different cutting parameters were investigated.

The measured temperature changes in the cutting zone resulting from the milling tests are presented in Figure 6.

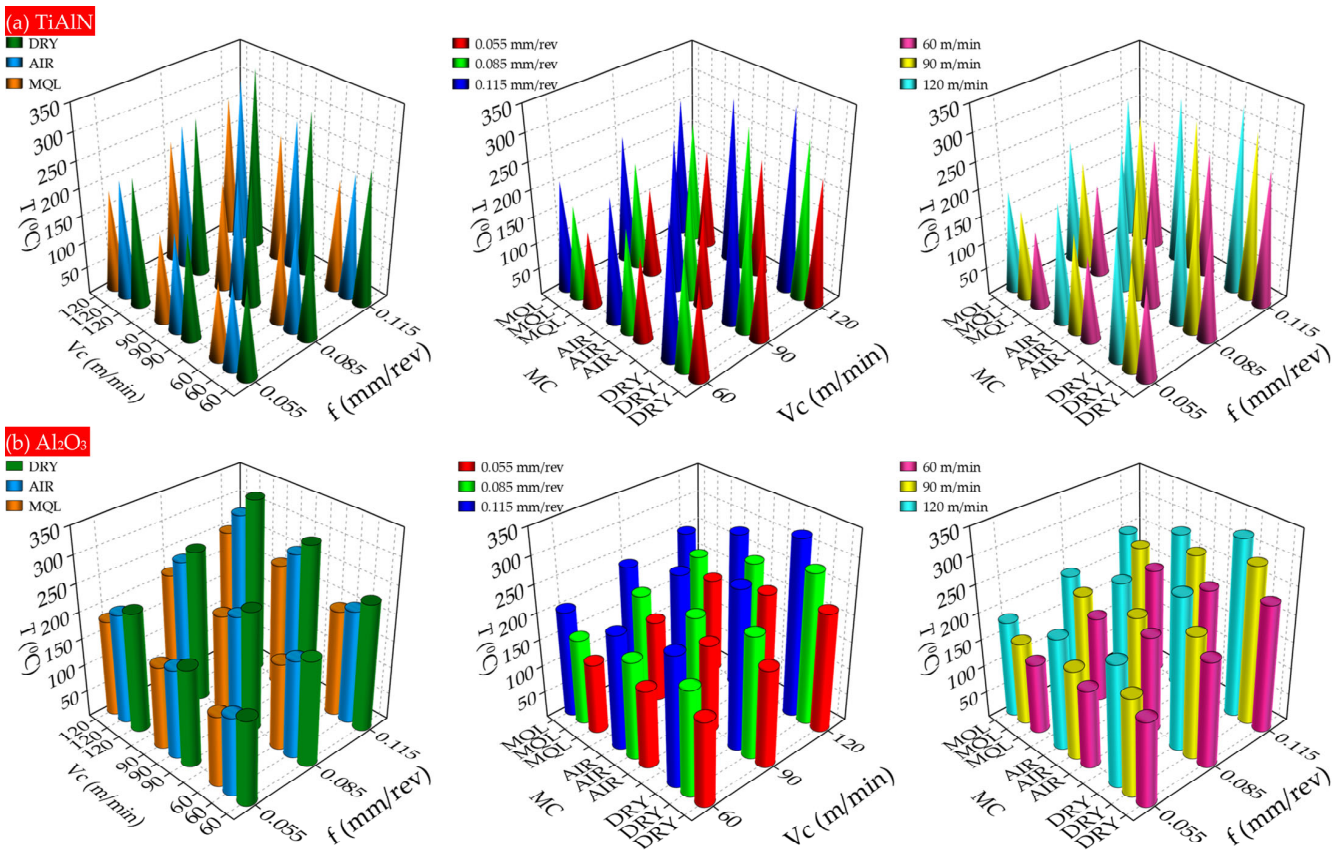


Figure 6. Cutting temperature results for different coating and machining conditions.

Figure 6 shows that the cutting temperature ranged from 129 °C to 338 °C for all milling tests. Using an Al_2O_3-coated tool, under MQL conditions, the minimum cutting temperature was recorded at 129 °C at a cutting speed of 60 m/min and a feed rate of 0.055 mm/rev. In contrast, under dry machining conditions, using a TiAlN-coated tool, the maximum cutting temperature was observed at 338 °C at a cutting speed of 120 m/min and a feed rate of 0.115 mm/rev. It was observed that cutting temperatures increased with increasing cutting speed and feed rate for both cutting tools and all machining conditions. However, it can be said that the most influential parameter on cutting temperature is the feed rate. Increasing the feed rate increases the unformed chip thickness and increases friction at the tool/workpiece interface, resulting in higher cutting temperatures in the cutting zone. It has been clearly stated that increased plastic deformation of the workpiece due to increased cutting speed is responsible for the temperature increase in the cutting zone [39,53].

In tests conducted with TiAlN-coated tools under dry machining conditions, the average cutting temperature was calculated to be 248.3 °C. The cutting temperature in air and MQL machining conditions decreased by 8.23% and 19.78%, respectively, compared to the dry machining conditions. Similarly, for the Al_2O_3-coated tool under dry machining conditions, the average cutting temperature was calculated to be 233.78 °C. The cutting temperature in air and MQL machining conditions decreased by 9.6% and 19.88%, respectively, compared to the dry machining conditions. In machining tests conducted with both cutting tools, the minimum cutting temperature was achieved with MQL machining, followed by air machining. Under the MQL machining condition, the coolant sprayed into the cutting

zone reduces friction at the tool-chip interface and cools the cutting zone. This resulted in a decrease in cutting temperature. In machining tests conducted with high air pressure, it was determined that air also reduced the heat generated in the cutting zone.

In machining tests conducted with TiAlN-coated tools under all cutting parameters and machining conditions, the average cutting temperature was calculated as 225.15 °C. In machining tests conducted with Al_2O_3-coated tools, the cutting temperature decreased by 6.27% compared to the TiAlN-coated tool, reaching 211.04 °C. This is thought to be due to the thermal conductivity and friction coefficients of the cutting tools used in the machining tests. The thermal conductivity (13 W/m °C) and coefficient of friction (0.29–0.39) of the CVD-Al_2O_3-coated cutting tool are lower than the thermal conductivity (15.4 W/m·°C) and coefficient of friction (0.5–0.7) of the PVD-TiAlN-coated cutting tool [54–56]. Lower thermal conductivity directs cutting heat to the chip and workpiece rather than the cutting tool. In this case, the heat generated in the cutting zone is dissipated away from the cutting zone by the chip, resulting in lower cutting temperatures [57,58].

The effects of cutting parameters, machining conditions, and cutting tool coatings on cutting temperature were determined using an ANOVA analysis. The ANOVA analysis results are shown in Table 8. As shown in Table 8, the most influential parameter on cutting temperature was the feed rate with a contribution of 49%, followed by cutting speed with 30.79%, machining conditions with 15.30%, and cutting tool coating with 2.02%.

Table 8. Cutting temperature analysis of variance (ANOVA) results.

Cutting Parameters	DF	Seq SS	Adj SS	Adj MS	F-Value	*p*-Value	Contribution (%)
CT	1	2688	2688	2688.2	32.29	0.000	2.02
MC	2	20,321	20,321	10,160.5	122.05	0.000	15.30
Vc (m/min)	2	40,879	40,879	20,439.6	245.51	0.000	30.79
f (mm/rev)	2	65,061	65,061	32,530.3	390.74	0.000	49.00
Error	46	3830	3830	83.3			2.88
Total	53	132,779					100.00

3.5. Evaluation of Tool Wear

The tool wear test results are shown in Figure 7. As expected, the maximum tool wear was measured as 339 µm at a chip volume of 7500 mm^3 under dry machining conditions with a TiAlN tool. It was observed that tool wear significantly decreased as the volume of removed chips increased in parallel with changes in machining conditions. In tests conducted with the TiAlN tool under air and MQL machining conditions, tool wear was reduced by 2.95% and 7.96%, respectively, compared to dry machining conditions. In the wear tests performed with the Al_2O_3 tool, the maximum wear amount was measured as 334 µm at a chip volume of 9000 mm^3 under dry machining conditions. In tests conducted with Al_2O_3 tools under air and MQL machining conditions, tool wear was reduced by 5.3% and 9%, respectively, compared to dry machining. The wear test results conducted with both tools under air machining conditions were observed to be better than those under dry machining conditions. This improvement is attributed to the 6 bar compressed air applied to the cutting zone, which likely reduced the cutting temperature and thereby reduced tool wear. In wear tests conducted with both cutting tools, the lowest tool wear was measured under MQL machining conditions. The cutting fluid used in MQL machining adheres and penetrates more effectively to the tool-chip interface. This has been reported to reduce tool wear by forming a thin lubricating film at the tool-chip interface, which decreases friction and cutting temperature [59]. It can be seen in Figure 7 that the wear test results obtained

with the Al_2O_3 tool under all machining conditions were better than those obtained with the TiAlN tool. This can be attributed to the lower coefficient of friction (0.29–0.39) [55] of the Al_2O_3 tool compared to that of the TiAlN tool (0.5–0.7) [56]. A low coefficient of friction reduces friction at the tool-chip interface. Therefore, cutting temperature and cutting forces decrease, which in turn delays tool wear.

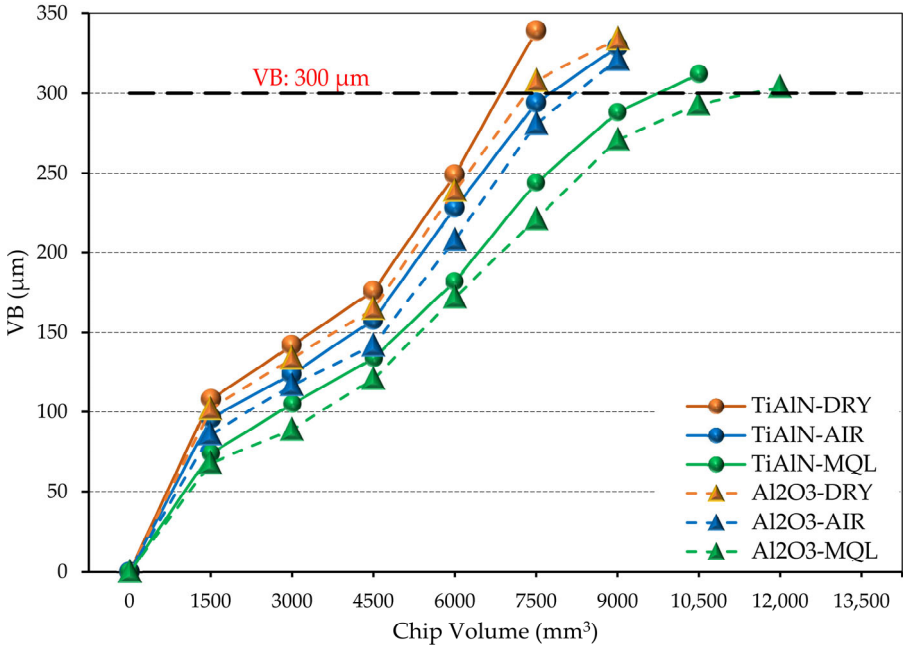


Figure 7. Tool wear values in different coatings and machining conditions.

Figure 8 shows SEM images of cutting tools resulting from tool wear tests, and Table 9 shows the results of EDS analyses. As illustrated in Figure 8, during dry machining tests with both cutting tools, the increase in mechanical loads and cutting temperature led initially to the formation of cracks on the tool surfaces. As the tests progressed, these cracks propagated and eventually resulted in tool fracture and severe wear. Figure 8 reveals tool damage such as built-up edges (BUEs), built-up layers (BULs), flank wear, coating peeling, and micro-chipping. Due to friction at the tool-chip interface, surface atoms adhere to each other (adhesion), resulting in an adhesion wear mechanism [60]. It has been observed that this wear mechanism significantly contributes to the formation of BUEs and BULs on the cutting tool, particularly in the machining of ductile alloys such as aluminum and titanium [61]. BUEs formed on the tool can be relatively hard and large in size. In some cases, they can take over the cutting process by replacing the tool edge. BUEs can be observed on any cutting tool when machining titanium alloys [62,63]. The BUEs and BULs formed on the cutting tool are also confirmed by the EDS analyses presented in Table 9. As observed in this study, the size and number of BUEs and BULs were greater in dry machining tests with both cutting tools. When the machining conditions were changed to air for both cutting tools, a reduction in the formation of BUEs and BULs was observed. One of the most significant properties of Ti6Al4V material is its low thermal conductivity [64]. It has been observed that the reduction in cutting temperature with air cooling reduces the formation of BUEs and BULs. Finally, during MQL machining, the oil film formed at the tool-chip interface reduces friction and provides effective cooling, thereby minimizing the tendency for BUE and BUL formation on both cutting tools. Additionally, it was observed that the coefficient of friction of the Al_2O_3-coated tool was lower than that of the TiAlN-coated tool, which resulted in lower BUE and BUL values on the Al_2O_3-coated tool. The high pressure and temperature generated during the machining of the Ti6Al4V alloy can

cause the workpiece material to weld to the tool surface. This repeated, unbalanced, high-friction force can cause the chip to rupture along with the flowing chip. When the tensile strength of the welded material exceeds the strength of the tool material, delamination or tearing can occur in the coating or substrate. This triggers adhesion wear, activating mechanisms that lead to increased surface damage. Therefore, adhesion and adhesion-induced damage are the result of the combined mechanical-thermal effect at the tool-chip interface [59,65]. In addition, previous studies have reported that the properties of the Ti6Al4V alloy, such as its low thermal conductivity, high specific cutting resistance, and tendency to stick, increase flank wear during the milling of this alloy [66].

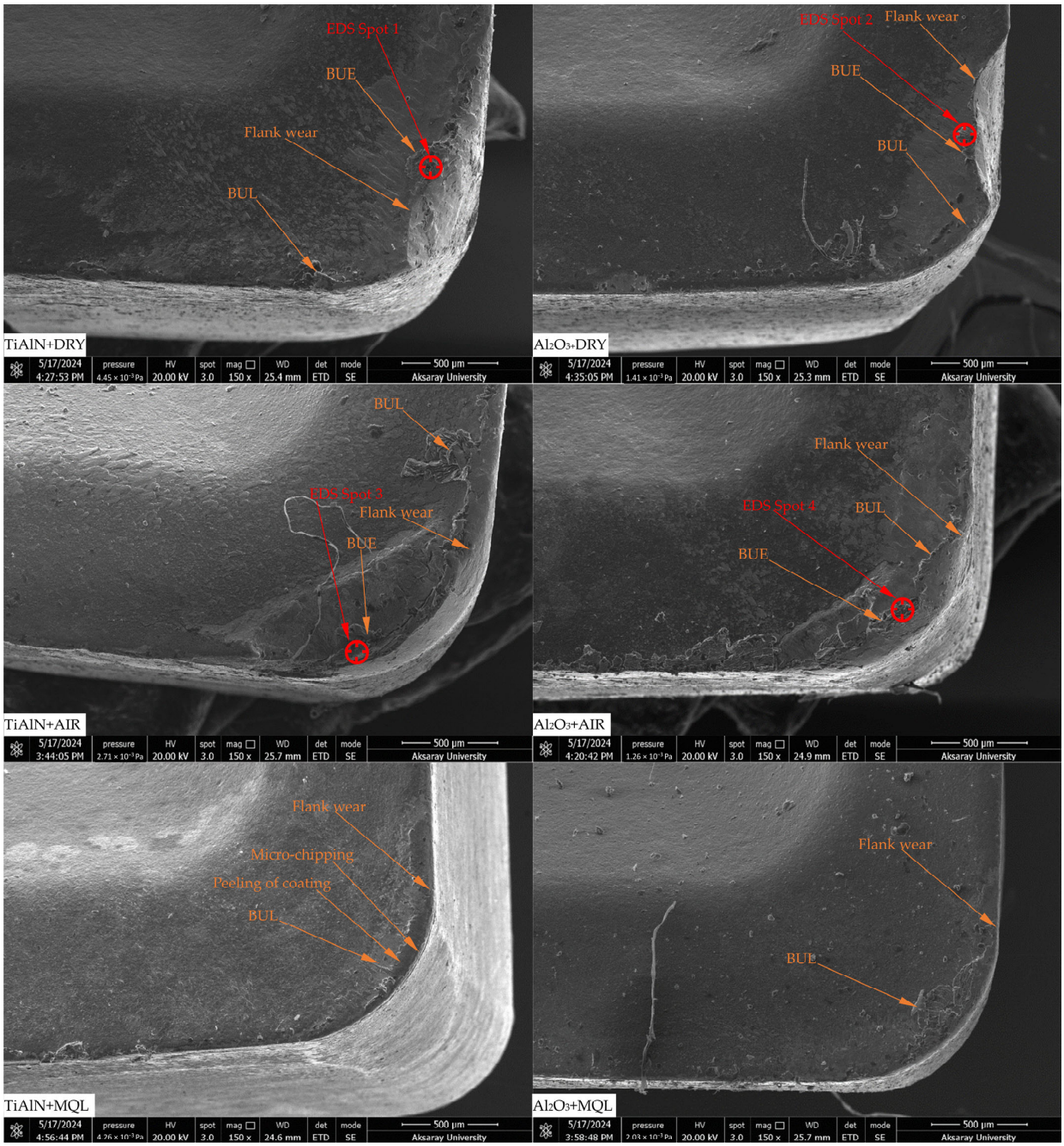


Figure 8. SEM image of worn tools in different coatings and machining conditions.

Table 9. EDS analysis results obtained from the cutting tools.

EDS Spot	Element Weights (%)						
	C	**Al**	**Si**	**Sn**	**Ti**	**V**	**Fe**
1	28.13	4.31	0.07	0.37	63.31	3.70	0.11
2	27.31	3.96	0.11	0.28	64.06	4.20	0.08
3	26.97	5.12	0.04	0.41	65.26	2.16	0.04
4	29.54	3.88	0.09	0.32	63.05	2.99	0.13

4. Conclusions

This study aimed to investigate the effects of cutting parameters, cutting tool coating, and machining conditions on cutting force, energy consumption, surface roughness, cutting temperature, and tool wear in the sustainable manufacturing of the Ti6Al4V alloy. The results obtained in this context are listed below:

- The lowest cutting force of 228.33 N was achieved using an Al_2O_3-coated tool at a cutting speed of 120 m/min, a feed rate of 0.055 mm/rev, and under MQL machining conditions. According to ANOVA analysis, the feed rate was the most influential parameter on cutting force, with a contribution of 74.81%.
- In the machining tests, the minimum energy consumption was measured as 2.694 J/mm^3 using an Al_2O_3-coated tool at a cutting speed of 120 m/min, a feed rate of 0.115 mm/rev, and under MQL conditions. ANOVA results showed that cutting speed was the most significant factor affecting energy consumption, accounting for 46.73%.
- The best surface finish was obtained with an Al_2O_3-coated tool under MQL conditions at a cutting speed of 120 m/min and a feed rate of 0.055 mm/rev, yielding a surface roughness of 0.402 µm. The feed rate was found to be the most effective parameter on surface roughness, with a contribution ratio of 70.13%.
- The minimum cutting temperature (129 °C) was recorded using an Al_2O_3-coated tool under MQL conditions at a cutting speed of 60 m/min and a feed rate of 0.055 mm/rev. According to ANOVA analysis, the feed rate (49%) and cutting speed (30.79%) were the most influential parameters affecting cutting temperature.
- The MQL machining condition proved to be the most effective, followed by air and then dry machining conditions. Owing to its superior lubrication and cooling characteristics, MQL significantly reduced cutting force, energy consumption, temperature, and tool wear.
- The CVD Al_2O_3-coated cutting tool outperformed the PVD TiAlN-coated tool across all performance indicators, providing lower cutting force and energy consumption, better surface quality, lower cutting temperatures, and enhanced tool wear resistance.
- SEM and EDX analyses revealed that wear mechanisms such as built-up edges (BUEs), built-up layers (BULs), and flank wear were predominant, particularly under dry machining conditions. MQL effectively reduced adhesion-related wear due to the formation of a lubricating oil film at the tool–chip interface.
- Tool wear was found to be lowest under MQL conditions for both cutting tools. The Al_2O_3-coated tool exhibited 9% less wear under MQL compared to dry machining, confirming its superior wear resistance attributed to lower friction coefficients.
- The low thermal conductivity of the Al_2O_3-coated cutting tool helped mitigate thermal damage by directing heat towards the chip and workpiece rather than the tool itself, thereby contributing to extended tool life and lower cutting temperatures.

Author Contributions: Conceptualization, B.Ö., H.B.U. and F.K.; methodology, B.Ö., H.B.U. and F.K.; software, B.Ö., H.B.U. and F.K.; validation, B.Ö., H.B.U. and F.K.; investigation, B.Ö., H.B.U. and F.K.; resources, B.Ö., H.B.U. and F.K.; data curation, B.Ö., H.B.U. and F.K.; writing—original draft preparation, B.Ö., H.B.U. and F.K.; writing—review and editing, B.Ö., H.B.U. and F.K.; visualization, B.Ö., H.B.U. and F.K.; supervision, B.Ö., H.B.U., and F.K. All authors have read and agreed to the published version of the manuscript.

Funding: This research received no external funding.

Data Availability Statement: The original contributions presented in this study are included in the article; further inquiries can be directed to the corresponding authors.

Conflicts of Interest: The authors declare no conflicts of interest.

Abbreviations

The following abbreviations are used in this manuscript:

Vc	Cutting speed
f	Feed rate
ap	Depth of cut
MQL	Minimum Quantity Lubrication
MC	Machining Conditions
BUE	Built-Up Edge
BUL	Built-Up Layer
Vb	Flank wear
SEM	Scanning Electron Microscope
EDX	Energy-Dispersive X-Ray Analysis

References

1. Peters, M.; Kumpfert, J.; Ward, C.H.; Leyens, C. Titanium alloys for aerospace applications. *Adv. Eng. Mater.* **2003**, *5*, 419–427. [CrossRef]
2. Ni, C.; Zhu, J.; Zhang, B.; An, K.; Wang, Y.; Liu, D.; Lua, W.; Zhucand, L.; Liu, C. Recent advance in laser powder bed fusion of Ti–6Al–4V alloys: Microstructure, mechanical properties and machinability. *Virtual Phys. Prototyp.* **2025**, *20*, e2446952. [CrossRef]
3. Qu, Z.; Zhang, Z.; Liu, R.; Xu, L.; Zhang, Y.; Li, X.; Zhao, Z.; Duan, Q.; Wang, S.; Li, S.; et al. High fatigue resistance in a titanium alloy via near-void-free 3D printing. *Nature* **2024**, *626*, 999–1004. [CrossRef]
4. Zhao, D.P.; Tang, J.C.; Nie, H.M.; Zhang, Y.; Chen, Y.K.; Zhang, X.; Li, H.X.; Yan, M. Macro-micron-nano-featured surface topography of Ti-6Al-4V alloy for biomedical applications. *Rare Met.* **2018**, *37*, 1055–1063. [CrossRef]
5. Chi, Y.; Dong, Z.; Cui, M.; Shan, C.; Xiong, Y.; Zhang, D.; Luo, M. Comparative study on machinability and surface integrity of γ-TiAl alloy in laser assisted milling. *J. Mater. Res. Technol.* **2024**, *33*, 3743–3755. [CrossRef]
6. Manepalli, S.; Purushothaman, S.; Maddula, S.S.; Bhagavathi, L.R.; Mamilla, R.S. Numerical modelling and simulation studies of laser beam heating parameters on depth of cut and surface temperature in laser-assisted machining of Ti6Al4V. *J. Micromanuf.* **2024**, 25165984241281015. [CrossRef]
7. Lu, H.; Wang, Z.; Cai, J.; Xu, X.; Luo, K.; Wu, L.; Lu, J. Effects of laser shock peening on the hot corrosion behaviour of the selective laser melted Ti6Al4V titanium alloy. *Corros. Sci.* **2021**, *188*, 109558. [CrossRef]
8. Al-Rubaie, K.S.; Melotti, S.; Rabelo, A.; Paiva, J.M.; Elbestawi, M.A.; Veldhuis, S.C. Machinability of SLM-produced Ti6Al4V titanium alloy parts. *J. Manuf. Process.* **2020**, *57*, 768–786. [CrossRef]
9. Veiga, C.; Davim, J.P.; Loureiro, A.J.R. Review on machinability of titanium alloys: The process perspective. *Rev. Adv. Mater. Sci.* **2013**, *34*, 148–164.
10. Seid Ahmed, Y.; Ryon, A. Tribological performance of a hybrid CryoMQL system on Ti6Al4V milling. *Int. J. Adv. Manuf. Technol.* **2022**, *120*, 8185–8199. [CrossRef]
11. An, Q.; Chen, J.; Tao, Z.; Ming, W.; Chen, M. Experimental investigation on tool wear characteristics of PVD and CVD coatings during face milling of Ti6242S and Ti-555 titanium alloys. *Int. J. Refract. Met. Hard Mater.* **2020**, *86*, 105091. [CrossRef]
12. Abdullah, R.I.R.; Redzuwan, B.I.; Aziz, M.S.A.; Kasim, M.S. Comparative study of tool wear in milling titanium alloy (Ti-6Al-4V) using PVD and CVD coated cutting tool. *Ind. Lubr. Tribol.* **2017**, *69*, 363–370. [CrossRef]

13. Yuan, S.M.; Yan, L.T.; Liu, W.D.; Liu, Q. Effects of cooling AIR temperature on cryogenic machining of Ti–6Al–4V alloy. *J. Mater. Process. Technol.* **2011**, *211*, 356–362. [CrossRef]
14. Gajrani, K.K. Assessment of cryo-MQL environment for machining of Ti-6Al-4V. *J. Manuf. Process.* **2020**, *60*, 494–502. [CrossRef]
15. Sahoo, S.P.; Datta, S.; Roy, T.; Ghosh, S. Machining performance of Ti6Al4V under DRY environment, pressurized AIR supply and water-MQL: Analysis of machining-induced vibration signals and captured thermographs. *Sādhanā* **2021**, *46*, 208. [CrossRef]
16. Saravanan, P.; Raj, D.S.; Hussain, S.; Shankar, V.R.; Raj, N. Optimization of jet position and investigation of the effects of multijet MQCL during end milling of Ti-6Al-4V. *J. Manuf. Process.* **2021**, *64*, 392–408. [CrossRef]
17. Jamil, M.; Zhao, W.; He, N.; Gupta, M.K.; Sarikaya, M.; Khan, A.M.; Sanjay, M.R.; Suchart, S.; Pimenov, D.Y. Sustainable milling of Ti–6Al–4V: A trade-off between energy efficiency, carbon emissions and machining characteristics under MQL and cryogenic environment. *J. Clean. Prod.* **2021**, *281*, 125374. [CrossRef]
18. An, Q.; Cai, C.; Zou, F.; Liang, X.; Chen, M. Tool wear and machined surface characteristics in side milling Ti6Al4V under DRY and supercritical CO2 with MQL conditions. *Tribol. Int.* **2020**, *151*, 106511. [CrossRef]
19. Ramesh, S.; Karunamoorthy, L.; Senthilkumar, V.S.; Palanikumar, K. Experimental study on machining of titanium alloy (Ti64) by CVD and PVD coated carbide inserts. *Int. J. Manuf. Technol. Manag.* **2009**, *17*, 373–385. [CrossRef]
20. Shokrani, A.; Al-Samarrai, I.; Newman, S.T. Hybrid cryogenic MQL for improving tool life in machining of Ti-6Al-4V titanium alloy. *J. Manuf. Process.* **2019**, *43*, 229–243. [CrossRef]
21. Cai, C.; Liang, X.; An, Q.; Tao, Z.; Ming, W.; Chen, M. Cooling/lubrication performance of DRY and supercritical CO2-based minimum quantity lubrication in peripheral milling Ti-6Al-4V. *Int. J. Precis. Eng. Manuf. Green Technol.* **2021**, *8*, 405–421. [CrossRef]
22. Bandapalli, C.; Sutaria, B.M.; Bhatt, D.V.P.; Singh, K.K. Tool wear analysis of micro end mills-uncoated and PVD coated TiAlN & AlTiN in high-speed micro milling of titanium alloy-Ti-0.3 Mo-0.8 Ni. *Procedia CIRP* **2018**, *77*, 626–629.
23. Park, K.H.; Yang, G.D.; Suhaimi, M.A.; Lee, D.Y.; Kim, T.G.; Kim, D.W.; Lee, S.W. The effect of cryogenic cooling and minimum quantity lubrication on end milling of titanium alloy Ti-6Al-4V. *J. Mech. Sci. Technol.* **2015**, *29*, 5121–5126. [CrossRef]
24. Rotella, G.; Dillon, O.W., Jr.; Umbrello, D.; Settineri, L.; Jawahir, I.S. The effects of cooling conditions on surface integrity in machining of Ti6Al4V alloy. *Int. J. Adv. Manuf. Technol.* **2014**, *71*, 47–55. [CrossRef]
25. Bai, X.; Li, C.; Dong, L.; Yin, Q. Experimental evaluation of the lubrication performances of different nanofluids for minimum quantity lubrication (MQL) in milling Ti-6Al-4V. *Int. J. Adv. Manuf. Technol.* **2019**, *101*, 2621–2632. [CrossRef]
26. Şirin, Ş.; Sarıkaya, M.; Yıldırım, Ç.V.; Kıvak, T. Machinability performance of nickel alloy X-750 with SiAlON ceramic cutting tool under DRY, MQL and hBN mixed nanofluid-MQL. *Tribol. Int.* **2021**, *153*, 106673. [CrossRef]
27. Monroy Vazquez, K.P.; Giardini, C.; Ceretti, E. Cutting force modeling. In *CIRP Encyclopedia of Production Engineering*; Springer: Berlin/Heidelberg, Germany, 2018; pp. 1–16.
28. Kalpakjian, S.; Schmid, S.R. *Manufacturing Engineering and Technology*, 7th ed.; Pearson: Mexico City, México, 2014.
29. Özlü, B.; Demir, H.; Türkmen, M.; Gündüz, S. Examining the machinability of 38MnVS6 microalloyed steel, cooled in different mediums after hot forging with the coated carbide and ceramic tool. *Proc. Inst. Mech. Eng. Part C J. Mech.* **2021**, *235*, 6228–6239. [CrossRef]
30. Özlü, B. Investigation of the effect of cutting parameters on cutting force, surface roughness and chip shape in turning of Sleipner cold work tool steel. *J. Fac. Eng. Archit. Gazi Univ.* **2021**, *36*, 1241–1251.
31. Özlü, B. Evaluation of energy consumption, cutting force, surface roughness and vibration in machining toolox 44 steel using taguchi-based gray relational analysis. *Surf. Rev. Lett.* **2022**, *29*, 2250103. [CrossRef]
32. Zou, Y.; Tang, S.; Guo, S.; Song, X. Tool wear analysis in turning inconel-657 using various tool materials. *Mater. Manuf. Process.* **2024**, *39*, 1363–1368. [CrossRef]
33. Vieira, J.M.; Machado, A.R.; Ezugwu, E.O. Performance of cutting fluids during face milling of steels. *J. Mater. Process. Technol.* **2001**, *116*, 244–251. [CrossRef]
34. Cicek, A.; Kıvak, T.; Ekici, E.; Kara, F.; Ucak, N. Performance of multilayer coated and cryo-treated uncoated tools in machining of AISI H13 tool steel—Part 1: Tungsten carbide end mills. *J. Mater. Eng. Perform.* **2021**, *30*, 3436–3445. [CrossRef]
35. Khanna, N.; Wadhwa, J.; Pitroda, A.; Shah, P.; Schoop, J.; Sarıkaya, M. Life cycle assessment of environmentally friendly initiatives for sustainable machining: A short review of current knowledge and a case study. *Sustain. Mater. Technol.* **2022**, *32*, e00413. [CrossRef]
36. Khanna, N.; Shah, P.; Wadhwa, J.; Pitroda, A.; Schoop, J.; Pusavec, F. Energy consumption and lifecycle assessment comparison of cutting fluids for drilling titanium alloy. *Procedia CIRP* **2021**, *98*, 175–180. [CrossRef]
37. Yıldırım, Ç.V.; Şirin, Ş.; Kıvak, T.; Ercan, H.; Sarıkaya, M. An attempt towards green machining of Ni-based Hastelloy C4 alloy: Effect of vegetable oils and their combination with TiO_2 and SiO_2 nanoparticles on outputs. *Sustain. Mater. Technol.* **2023**, *37*, e00668. [CrossRef]

38. Öztürk, B.; Kara, F. Multi-objective optimization of machinability and energy consumption of cast iron depending on cooling rate. *Machines* **2025**, *13*, 84. [CrossRef]
39. Akgün, M.; Özlü, B.; Kara, F. Effect of PVD-TiN and CVD-Al2O3 coatings on cutting force, surface roughness, cutting power, and temperature in hard turning of AISI H13 steel. *J. Mater. Eng. Perform.* **2023**, *32*, 1390–1401. [CrossRef]
40. Çelik, M.; Şencan, A.Ç.; Şirin, Ş.; Erdoğan, B.; Şencan, C. Effect of hBN and SDS added vegetable based cutting fluid application on the performance of turning Ti6Al4V alloys: A comparative analysis with Taguchi and ANN approaches. *Mater. Chem. Phys.* **2024**, *322*, 129552. [CrossRef]
41. Demir, H. The effects of microalloyed steel preheat treatment on microstructure and machinability. *Int. J. Adv. Manuf. Technol.* **2008**, *35*, 1041–1046. [CrossRef]
42. Akgün, M.; Demir, H.; Çiftçi, İ. Optimization of surface roughness in turning Mg2Si particle reinforced magnesium alloys. *J. Polytech.* **2018**, *21*, 645–650.
43. Ferreira, R.; Carou, D.; Lauro, C.H.; Davim, J.P. Surface roughness investigation in the hard turning of steel using ceramic tools. *Mater. Manuf. Process.* **2016**, *31*, 648–665. [CrossRef]
44. Demir, H.; Gündüz, S. The effects of aging on machinability of 6061 aluminium alloy. *Mater. Des.* **2009**, *30*, 1480–1483. [CrossRef]
45. Akgün, M. Measurement and optimization of cutting forces, surface roughness and temperature in turning of AZ91 Mg alloy. *Sādhanā* **2023**, *48*, 60. [CrossRef]
46. Binali, R. Experimental and machine learning comparison for measurement the machinability of nickel based alloy in pursuit of sustainability. *Measurement* **2024**, *236*, 115142. [CrossRef]
47. Davim, J.P.; Figueira, L. Machinability evaluation in hard turning of cold work tool steel (D2) with ceramic tools using statistical techniques. *Mater. Des.* **2007**, *28*, 1186–1191. [CrossRef]
48. Gaitonde, V.N.; Karnik, S.R.; Figueira, L.; Davim, J.P. Performance comparison of conventional and wiper ceramic inserts in hard turning through artificial neural network modeling. *Int. J. Adv. Manuf. Technol.* **2011**, *52*, 101–114. [CrossRef]
49. Kıvak, T. Optimization of surface roughness and flank wear using the Taguchi method in milling of Hadfield steel with PVD and CVD coated inserts. *Measurement* **2014**, *50*, 19–28. [CrossRef]
50. Storchak, M.; Stehle, T.; Möhring, H.C. Determination of thermal material properties for the numerical simulation of cutting processes. *Int. J. Adv. Manuf. Technol.* **2022**, *118*, 1941–1956. [CrossRef]
51. Hao, G.; Liu, Z. The heat partition into cutting tool at tool-chip contact interface during cutting process: A review. *Int. J. Adv. Manuf. Technol.* **2020**, *108*, 393–411. [CrossRef]
52. Kara, F. Investigation of the effect of Al_2O_3 nanoparticle-added MQL lubricant on sustainable and clean manufacturing. *Lubricants* **2024**, *12*, 393. [CrossRef]
53. Yıldırım, Ç.V.; Şirin, Ş.; Kıvak, T.; Sarıkaya, M. The effect of nanofluids reinforced with different surfactants on the machining and friction-wear properties of Waspaloy. *Tribol. Int.* **2023**, *181*, 108316. [CrossRef]
54. Zhang, J.; Zhang, G.; Fan, G. Effects of tool coating materials and coating thickness on cutting temperature distribution with coated tools. *Int. J. Appl. Ceram. Technol.* **2022**, *19*, 2276–2284. [CrossRef]
55. Jena, A.; Pattnaik, S.K.; Sarangi, S.K. Multi-spindle drilling tools used for DRY machining of aluminium. *J. Braz. Soc. Mech. Sci. Eng.* **2024**, *46*, 441. [CrossRef]
56. Aamir, M.; Tolouei-Rad, M.; Giasin, K. Multi-spindle drilling of Al2024 alloy and the effect of TiAlN and TiSiN-coated carbide drills for productivity improvement. *Int. J. Adv. Manuf. Technol.* **2021**, *114*, 3047–3056. [CrossRef]
57. Zhang, S.J.; Liu, Z.Q. Heat conduction analysis of coated cutting tools with temperature-dependent properties. *Adv. Mater. Res.* **2009**, *69*, 389–393. [CrossRef]
58. Balaji, A.K.; Mohan, V.S. An 'effective cutting tool thermal conductivity' based model for tool–chip contact in machining with multi-layer coated cutting tools. *Mach. Sci. Technol.* **2002**, *6*, 415–436. [CrossRef]
59. Şirin, E.; Yıldırım, Ç.V.; Şirin, Ş.; Kıvak, T.; Sarıkaya, M. Comprehensive analysis of cutting temperature, tool wear, surface integrity and tribological properties in sustainable milling of Ti6Al4V alloy: LN2, nanofluid and hybrid machining. *J. Manuf. Process.* **2024**, *131*, 1360–1371. [CrossRef]
60. Aghababaei, R. Effect of adhesion on material removal during adhesive wear. *Phys. Rev. Mater.* **2019**, *3*, 063604. [CrossRef]
61. Alparslan, C.; Bayraktar, Ş. Tool wear in machining of wrought and cast aluminium alloys: Literature review. *Manuf. Technol. Appl.* **2021**, *2*, 34–46. [CrossRef]
62. Fang, N.; Pai, P.S.; Mosquea, S. The effect of built-up edge on the cutting vibrations in machining 2024-T351 aluminum alloy. *Int. J. Adv. Manuf. Technol.* **2010**, *49*, 63–71. [CrossRef]
63. Zhang, C.; Zou, D.; Mazur, M.; Mo, J.P.; Li, G.; Ding, S. The state of the art in machining additively manufactured titanium alloy Ti-6Al-4V. *Materials* **2023**, *16*, 2583. [CrossRef] [PubMed]
64. Bermingham, M.J.; Sim, W.M.; Kent, D.; Gardiner, S.; Dargusch, M.S. Tool life and wear mechanisms in laser assisted milling Ti–6Al–4V. *Wear* **2015**, *322*, 151–163. [CrossRef]

65. Ding, F.; Wang, C.; Zhang, T.; Deng, Y.; Zhu, X. Adhesive wear mechanism of coated tools and its influence on cutting performance during machining of Zr-based bulk metallic glass. *J. Mater. Res. Technol.* **2023**, *27*, 5489–5506. [CrossRef]
66. Ezugwu, E.O.; Wang, Z.M. Titanium alloys and their machinability—A review. *J. Mater. Process. Technol.* **1997**, *68*, 262–274. [CrossRef]

Disclaimer/Publisher's Note: The statements, opinions and data contained in all publications are solely those of the individual author(s) and contributor(s) and not of MDPI and/or the editor(s). MDPI and/or the editor(s) disclaim responsibility for any injury to people or property resulting from any ideas, methods, instructions or products referred to in the content.